# Release of $Ca^{2+}$ from Individual Plant Vacuoles by Both $InsP_3$ and Cyclic ADP–Ribose

Gethyn J. Allen,* Shelagh R. Muir, Dale Sanders

Calcium mobilization from intracellular pools couples many stimuli to responses in plant cells. Cyclic adenosine 5′-diphosphoribose (cADPR), which interacts with a ryanodine receptor in certain animal cells, was shown to elicit calcium release at the vacuolar membrane of beet storage root. The vacuolar calcium release pathway showed similarities to cADPR-gated calcium release in animal cells, including inhibition by ruthenium red, ryanodine activation, and high affinity for cADPR [Michaelis constant ($K_m$) = 24 ± 7 nanomolar]. Analysis by patch-clamping demonstrated that the cADPR-gated pathway in beet is voltage-dependent over the physiological range, does not spontaneously desensitize, and is colocalized with an inositol 1,4,5-trisphosphate ($InsP_3$)–gated calcium release pathway in individual vacuoles.

Calcium-mediated intracellular signaling is ubiquitous in plants (*1*, *2*). Coupling of diverse stimuli such as red light (*3*), hormones (*4*), gravity (*5*), touch, cold shock, and fungal elicitors (*6*) to their respective specific responses involves elevation of cytosolic free $Ca^{2+}$. Stimulus specificity is most likely encoded through a multiplicity of $Ca^{2+}$ mobilization pathways, each with its own gating properties (*7*, *8*). The $Ca^{2+}$ mobilization properties of $InsP_3$ have been established in plants (*9*, *10*).

Ryanodine receptors are ion channels that control intracellular $Ca^{2+}$ mobilization in many mammalian cell types, where $Ca^{2+}$ release through these channels can augment $InsP_3$-elicited $Ca^{2+}$ mobilization (*7*). Interactions between these two discrete $Ca^{2+}$ release pathways are crucial to the generation of stimulus-specific spatiotemporal patterning of cytosolic $Ca^{2+}$ signals. The nicotinamide adenine dinucleotide ($NAD^+$) metabolite cADPR mobilizes $Ca^{2+}$ from internal stores (*11*) by activating at least one ryanodine receptor isoform (RYR2) (*12*–*14*).

To examine the possibility that cADPR-activated $Ca^{2+}$ mobilization occurs in plants, we prepared microsomes rich in vacuolar membrane from storage roots of red beet and loaded the microsomes with $Ca^{2+}$ by means of a $Ca^{2+}/H^+$ antiport, which was in turn driven by a pH gradient generated by the vacuolar $H^+$ adenosine triphosphatase (ATPase) (*15*). After termination of loading by addition of the uncoupler FCCP, addition of cADPR to a final concentration of 100 nM resulted in a significant $Ca^{2+}$ release amounting to 15 to 17% of the total uptake in comparison with controls (Fig. 1A). The cADPR-elicited release was inhibited 55 ± 8% ($n$ = 5) by 30 μM ruthenium red (Fig. 1A, inset), a diagnostic antagonist of ryanodine receptors (*16*). Ryanodine itself, which at 100 μM releases $Ca^{2+}$ from a cADPR-sensitive $Ca^{2+}$ pool in rat brain microsomes (*17*), also elicited $Ca^{2+}$ release from the beet microsomes (17% of accumulated $Ca^{2+}$) (Fig. 1B). Neither ruthenium red nor ryanodine (10 μM) affects $InsP_3$-elicited $Ca^{2+}$ release from beet microsomes (*18*). Pre-release of $Ca^{2+}$ by ryanodine precludes further $Ca^{2+}$ mobilization by cADPR (Fig. 1C), suggesting that the two ligands release $Ca^{2+}$ from the same subpopulation of vesicles.

The limited extent (15 to 17%) to which cADPR is able to mobilize $Ca^{2+}$ from beet microsomes is similar to the restricted $Ca^{2+}$ release that occurs with $InsP_3$ in this preparation (*19*), and quantitative arguments based on $InsP_3$-gated channel density in the native vacuolar membrane indicate that only ≈15% of vesicles will contain an $InsP_3$-gated channel, even if all vesicles are of vacuolar origin (*19*). Thus, limited $Ca^{2+}$ release is compatible with effective mobilization of all $Ca^{2+}$ in vesicles with a cADPR-gated channel.

The intracellular location of the response to cADPR was investigated and further characterized by patch-clamp of intact vacuoles from beet storage root. Of 24 vacuoles tested, all 15 (63%) that responded to cADPR did so with a significant and selective increase in the instantaneous inward current (current flowing into the cytosol from the vacuolar lumen) (*20*) (Fig. 2, A and B). The noncyclic analog of cADPR (adenosine 5′-diphosphoribose) had no effect on the current-voltage (*I*-*V*) relation in 10 vacuoles assayed (Fig. 2C). The voltage dependence of the cADPR-activated inward current is compatible with its appearance in vivo, where the transvacuolar membrane potential lies in the range −20 to −50 mV (*21*).

The concentration dependence of the cADPR-activated current (Fig. 3) demonstrates that, as in mammalian (*22*) and invertebrate (*23*) cells, cADPR is active in the nanomolar concentration range. The Michaelis constant ($K_m$) for cADPR is independent of membrane voltage and lies in the range of 20 to 25 nM.

The ionic selectivity of the cADPR-gated current can be calculated from the mean reversal potential of +8.6 ± 2.4 mV (Fig.

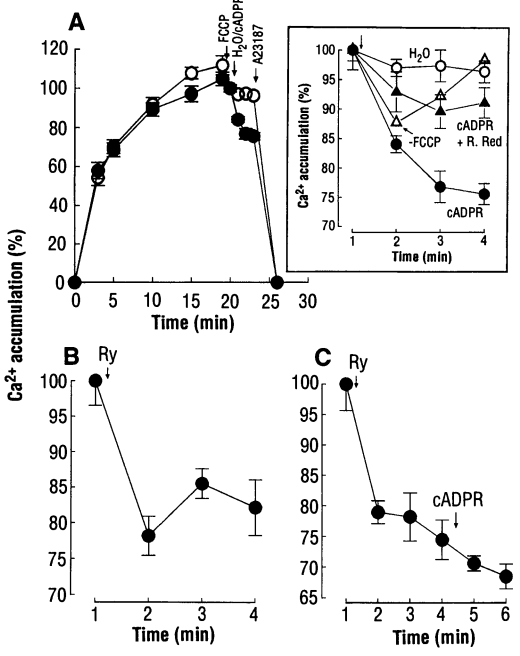


**Fig. 1.** Calcium release from vacuolar-enriched microsomes of beet by cADPR. (**A**) Loading (*31*) of $^{45}Ca^{2+}$ into the vesicles was terminated by addition of the uncoupler FCCP to a final concentration of 10 μM. Curves are standardized to this point [100% = 6.9 ± 0.2 (5) nmol $mg^{-1}$]. Subsequently, either 100 nM (final concentration) cADPR (●) or an equivalent volume of $H_2O$ (○) was added at the time indicated. Finally, addition of the $Ca^{2+}$ ionophore A23187 (5 μM final concentration) collapsed the remaining $Ca^{2+}$ gradient. (**Inset**) $Ca^{2+}$ release from (A) shown on a magnified scale. Each point is the mean ± SEM of five replicates. Also shown is cADPR-elicited $Ca^{2+}$ release from identical experiments in the presence of 30 μM ruthenium red (▲) and reuptake of released $Ca^{2+}$ in the absence of FCCP (△) (one of seven similar replicates). (**B**) As in (A) ($Ca^{2+}$ release shown), except that 100 μM (final concentration) ryanodine was added at the time indicated. Each point is the mean ± SEM of four replicates [100% = 7.2 ± 0.4 (*4*) nmol $mg^{-1}$]. (**C**) As in (B), except that addition of 100 μM (final concentration) ryanodine was followed by cADPR at 100 nM (final concentration) as indicated. Each point is the mean ± SEM of five replicates [100% = 6.4 ± 0.4 (5) nmol $mg^{-1}$].

The Plant Laboratory, Biology Department, University of York, Post Office Box 373, York YO1 5YW, UK.

*To whom correspondence should be addressed.

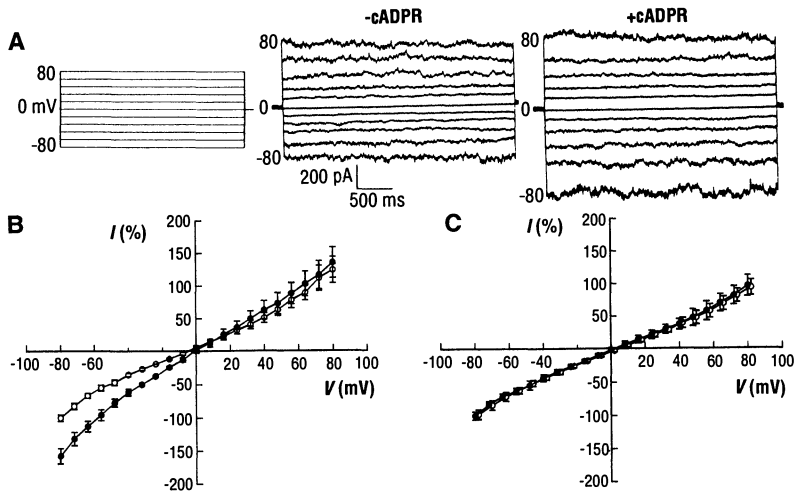


**Fig. 2.** Membrane currents elicited by cADPR across intact red beet vacuoles (*32*). (**A**) Effect of 100 nM cADPR on vacuolar membrane currents obtained with whole-vacuole mode patch-clamp. Voltage was held at 0 mV and stepped to ±80 mV in 8-mV steps. Potentials and currents are referenced to the luminal medium (*20*). The bath (cytosolic) medium contained 200 mM KCl, 1 mM $CaCl_2$, 5 mM tris-MES (pH 7.5), 200 μM $ZnCl_2$, and 600 mM sorbitol. The pipette (luminal) medium contained an identical solution, except that $CaCl_2$ was increased to 5 mM, the pH was 5.5, and $Zn^{2+}$ was omitted. $E_L$ was negligible (<1 mV) with these solutions. (**B**) Steady-state *I-V* relations of whole vacuoles sampled 500 ms after onset of each voltage pulse in the absence (○) or presence (●) of 100 nM cADPR. Currents are normalized to the current at −80 mV in the absence of cADPR (100% = 36 ± 7 mA $m^{-2}$). Fast vacuolar channel activity, which is normally responsible for much of the inward current (*28*), is inhibited by the high bath $Ca^{2+}$ concentration, and slow vacuolar channel activity, responsible for outward current, is inhibited by $Zn^{2+}$ (*9*). This reduces background conductance to an ohmic leak (○) against which subsequent changes can be measured. Points are the means ± SD from four vacuoles. (**C**) As in (B), but with addition of 100 nM of the noncyclic analog of cADPR that fails to elicit a membrane current. Points are the means ± SD from 10 vacuoles. Points with noncyclic ADPR have been offset by 2 mV to aid resolution of the curves.

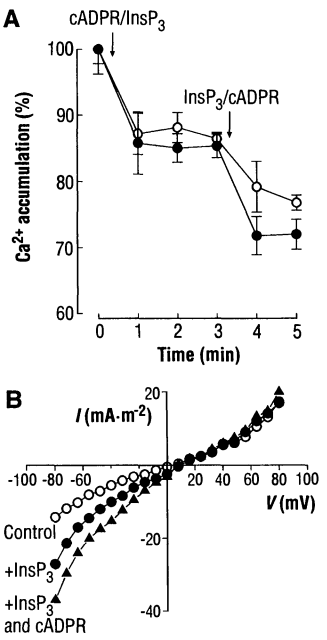


**Fig. 4.** Additive $Ca^{2+}$ release from beet vacuoles by saturating doses of cADPR and $InsP_3$. (**A**) $Ca^{2+}$ release from vacuolar-enriched microsomes was initiated first by addition of 100 nM cADPR, then 10 μM $InsP_3$ (●) or with these two ligands added in reverse order (○). Data are the means ± SEM of five replicates for each sequence. Other conditions are as Fig. 1. (**B**) Additive nature of $InsP_3$- and cADPR-induced currents in a single vacuole. Whole-vacuole *I-V* relations were recorded before the addition of ligands (○), after the addition of 1 μM $InsP_3$ (●), and after the addition of 100 nM cADPR in the continued presence of $InsP_3$ (▲). Data are from a representative vacuole; similar results were obtained in seven out of nine vacuoles that maintained constant seal resistance during the experiment.

**Fig. 3.** Dose dependence of cADPR-induced currents. (**A**) Steady-state *I-V* difference relations of patch-clamped beet vacuoles in response to addition of cADPR at 12.5 nM (△), 25 nM (▲), 50 nM (○), 100 nM (●), or 150 nM (□). Currents induced by cADPR rectify in the inward direction. Points are the means ± SEM from 2, 3, or 5 vacuoles at each cADPR concentration. Other conditions are as in Fig. 2. The mean reversal potential was +8.6 ± 2.4 mV; this was used to calculate the selectivity of the current as described in (*33*). (**B**) Current densities at -40 (○) and -80 mV (●) from (A) as a function of cADPR concentration. Solid lines are nonlinear least squares fits of Michaelis-Menten functions to each data set, which yields $K_m$ values for cADPR of 22 ± 7 and 25 ± 6 nM at −40 and −80 mV, respectively.

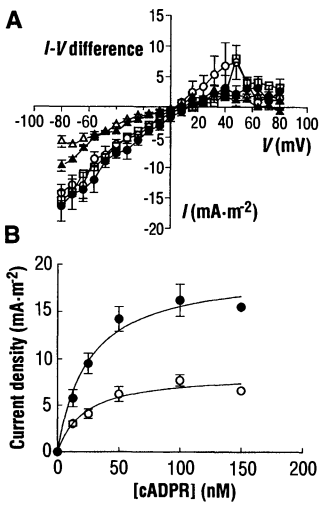


3A). The resultant selectivity ratio for $Ca^{2+}$ against $K^+$ lies between 9:1 and 27:1. Thus, although the luminal activities of $Ca^{2+}$ and $K^+$ are typically in the region of 5 mM and 200 mM, respectively (*24*), the equilibrium potential for $Ca^{2+}$ ($E_{Ca}$ = +130 mV) is considerably further displaced from the prevailing membrane potential than is the equilibrium potential for $K^+$ ($E_K$ = +28 mV). This difference in driving force will ensure that $Ca^{2+}$ carries the dominant component of the cADPR-gated inward current. These results indicate that cADPR mobilizes $Ca^{2+}$ in plant cells and that the selectivity of the current is similar to that of ryanodine-gated channels in animal cells (*25*).

The way in which $InsP_3$ and ryanodine receptors interact to produce a $Ca^{2+}$ signaling phenotype has been the subject of intense speculation (*7*). According to the "two-store" model (*26*) developed to explain $Ca^{2+}$ spiking in animal cells, each receptor accesses separate $Ca^{2+}$ pools that can fill and empty independently, but that communicate through changes in cytosolic $Ca^{2+}$ concentration. In beet microsomes, saturating concentrations of $InsP_3$ and cADPR release accumulated $Ca^{2+}$ in an additive fashion (Fig. 4A) indicating that the two ligands act independently on $Ca^{2+}$ release. The data could be interpreted to indicate that the two ligands interact with separate intracellular pools or that individual vacuoles fragment into many smaller vesicles some of which may have only one pathway.

Patch-clamp analysis of intact vacuoles supports this latter explanation by demonstrating that both the $InsP_3$- and cADPR-mobilizable pathways can reside in a single vacuole. Addition of a saturating concentration of $InsP_3$ induced a selective shift in the steady-state inward current, and the subsequent addition of a saturating concentration of cADPR in the continued presence of $InsP_3$ yielded a further increment in the inward current at negative potentials (Fig. 4B). The cADPR-activated current was smaller (58 ± 11% at −80 mV; $n$ = 7) than

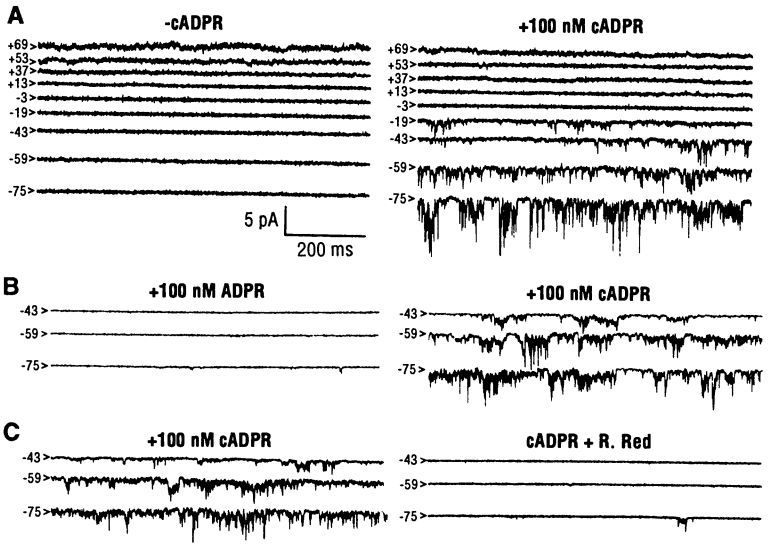


**Fig. 5.** Single-channel events induced by cADPR. (**A**) Currents recorded from a cytosolic-side-out patch in the absence and presence of cADPR in the bath. (**B**) Control patch demonstrating the dependence of channel activity on the cyclic isomer of ADPR. (**C**) Channel inhibition by 100 μM ruthenium red in the bath. In all experiments the solutions were as in Fig. 2, except that the pipette:bath $CaCl_2$ gradient was increased to 50 mM:5 mM. (A), (B), and (C) are from separate patches. Holding potentials indicated are corrected for an $E_L$ of −3 mV.

the $InsP_3$-activated current.

Single-channel events could be measured in cytosolic-side-out membrane patches after addition of cADPR to the bath solution (Fig. 5). Channel activity occurred over the physiological potential range (Fig. 5A), was dependent on the cyclic isomer of ADPR (Fig. 5B), and was inhibited by ruthenium red (Fig. 5C). Channel activity was observed in 26% (14/54) of patches suggesting a clustering of channels in the membrane. The single channels showed very rapid gating kinetics as also observed for cADPR activation of ryanodine receptors in planar lipid bilayers (*13*, *14*) and $InsP_3$-gated channels at the vacuolar membrane (*27*).

Ligand-activation of $Ca^{2+}$ release pathways will open $Ca^{2+}$-activated slow vacuolar (SV) cation channels in vivo, through both the elevation of cytosolic $Ca^{2+}$ (*28*) and the opening of $Ca^{2+}$-activated $K^+$ channels that depolarize the vacuolar membrane to positive values around $E_K$(*29*). The SV channel opens at depolarized potentials and its significant $Ca^{2+}$ permeability (*29*) suggests that it mediates $Ca^{2+}$-induced $Ca^{2+}$ release. Therefore, cADPR- and $InsP_3$-gated $Ca^{2+}$ release probably act as triggers of $Ca^{2+}$-induced $Ca^{2+}$ release. Spontaneous inactivation of cADPR-generated vacuolar currents was not observed, as is also the case for $InsP_3$ currents at this membrane (*9*, *27*). Furthermore, unlike in animal cells, termination of any ligand-generated $Ca^{2+}$ signal in plant cells cannot arise from depletion of internal stores because the vacuole typically occupies about 90% of the intracellular volume and contains millimolar concentrations of $Ca^{2+}$. Hence, it is probably the voltage dependence of ligand-gated $Ca^{2+}$ currents that ensures that $Ca^{2+}$ release through these channels is terminated until ligand metabolism deactivates the channels.

Our results suggest that cADPR signaling pathways are highly conserved among eukaryotes and that cADPR probably acts as a global signaling molecule, as does $InsP_3$. The presence of two classes of vacuolar ligand-gated $Ca^{2+}$ mobilization pathway, each of which could act coordinately with $Ca^{2+}$- and voltage-operated $Ca^{2+}$ release channels in the same membrane, would enhance the possibilities of generating a $Ca^{2+}$ signature specific for each stimulus.

## REFERENCES AND NOTES


1. S. Gilroy, P. C Bethke, R. L. Jones, *J. Cell Sci.* **106**, 453 (1993).
2. B. W. Poovaiah and A. S. N. Reddy, *Crit. Rev. Plant Sci.* **12**, 185 (1993).
3. C. Bowler, G. Neuhaus, H. Yamagata, N. H. Chua, *Cell* **77**, 73 (1994).
4. M. R. McAinsh, C. Brownlee, A. M. Hetherington, *Nature* **343**, 186 (1990).
5. C. A. Gehring, D. A Williams, S. H. Cody, R. W. Parish, *ibid.* **345**, 528 (1990).
6. M. R. Knight, A. K. Campbell, S. M. Smith, A. J. Trewavas, *ibid.* **352**, 524 (1991).
7. M. J. Berridge, *ibid.* **361**, 315 (1993).
8. E. Johannes, J. M. Brosnan, D. Sanders, *Philos. Trans. R. Soc. London Ser. B* **338**, 105 (1992).
9. J. Alexandre, J. P. Lassalles, R. T. Kado, *Nature* **343**, 567 (1990).
10. G. G. Coté and R. C. Crain, *BioEssays* **16**, 39 (1994).
11. D. L. Clapper, T. F. Walseth, P. J. Dargie, H. C, Lee, *J. Biol. Chem.* **262**, 9561 (1987); H. C. Lee *et al.*, *ibid.* **264**, 1608 (1989).
12. A. Galione, H. C. Lee, W. B. Busa, *Science* **253**, 1143 (1991).
13. L. G. Mészáros, J. Bak, A. Chu, *Nature* **364**, 76 (1993).
14. R. Sitsapesan, S. J. McGarry, A. J. Williams, *Circ. Res.* **75**, 596 (1994).
15. J. M. Brosnan and D. Sanders, *FEBS Lett.* **260**, 70 (1990).
16. A. Galione, *Mol. Cell. Endocrinol.* **98**, 125 (1994).
17. A. M. White, S. P. Watson, A. Galione, *FEBS. Lett.* **318**, 259 (1993).
18. E. Johannes, J. M. Brosnan, D. Sanders, *Plant J.* **2**, 97 (1992).
19. J. M. Brosnan, *Nature* **344**, 593 (1990).
20. A. Bertl *et al.*, *Science* **258**, 873 (1992).
21. P. A. Rea and D. Sanders, *Physiol. Plant.* **71**, 131 (1987).
22. S. Takasawa, K. Nata, H. Yonekura, H. Okamoto, *Science* **259**, 370 (1993).
23. H. C. Lee, *J. Biol. Chem.* **268**, 293 (1993).
24. G. J. Allen and D. Sanders, *Plant Cell* **6**, 685 (1994).
25. G. Meissner, *Annu. Rev. Physiol.* **56**, 485 (1994)
26. M. J. Berridge and A. Galione, *FASEB J.* **2**, 3074 (1988).
27. G. J. Allen and D. Sanders, *Plant J.* **6**, 687 (1994).
28. R. Hedrich and E. Neher, *Nature* **329**, 833 (1987).
29. J. Ward and J. I Schroeder, *Plant Cell* **6**, 669 (1994).
30. P. H. Barry and J. W. Lynch, *J. Membr. Biol.* **121**, 101 (1991).
31. Microsomes were prepared from storage roots of beet and loaded with $Ca^{2+}$ (*15*). Uptake was initiated by addition of microsomes (30 to 50 mg of protein) to 1 ml of assay medium [400 mM glycerol, 5 mM BTP-MES (pH 7.4), 50 mM KCl, 3 mM $MgSO_4$, 3 mM tris-ATP (adenosine triphosphate), 0.3 mM $NaN_3$, and 10 μM $^{45}CaCl_2$ (2.2 mCi $ml^{-1}$)] at 20°C. No subsequent additions contained more than 1% of the total assay volume. Aliquots (50 μl) were removed and filtered on prewetted nitrocellulose filters (0.45-μm pore diameter) and washed with 5 ml of ice-cold wash medium [400 mM glycerol, 0.2 mM $CaCl_2$, and 5 mM BTP-MES (pH 7.4)]. Radioactivity retained on the filters was determined by liquid scintillation counting. Radioactivity remaining on the filters after addition of A23187 was defined as nonaccumulated $Ca^{2+}$ and was subtracted from all data points; this correction never amounted to more than 25% of the overall maximum $Ca^{2+}$ accumulation.
32. Intact vacuoles were isolated from storage roots of red beet by a tissue-slicing procedure (*27*) and aspirated into the patch-clamp bath. Vacuole diameter was measured (±1.25 μm) and was in the range of 35 to 75 μm. Patch pipettes were pulled from thin-walled borosilicate glass capillaries (Kimax, Vineland, NJ), Sylgard coated (Dow Corning), and fire polished. Pipette resistance in the experimental solutions was 8 to 12 megohm. Vacuole-attached seals of 5 gigohm or greater were achieved after gentle suction through the pipette. Recordings were made as described (*27*) in the "whole vacuole" configuration after voltage pulses of up to 1 V were applied with an A310 accupulser (WPI, New Haven, CT). Cytosolic-side-out patches were formed by withdrawing the pipette from the vacuole after "whole vacuole" configuration had been achieved. The reference electrode was a Ag/AgCl half-cell connected through a 3% (w/v) agar bridge in pipette medium to the bath. Pipette potentials were controlled with an EPC-7 patch-clamp amplifier (List, Darmstadt, Germany). Data were digitized at 2 to 5 kHz (1401 AD converter, Cambridge Electronic Design) and recorded on computer for analysis. Currents were low-pass filtered at 0.5 to 1 kHz. Liquid junction potentials ($E_L$) were calculated as described in (*30*). Solutions were exchanged with two low-noise peristaltic pumps (Minipuls 3, Gilson), with exchange being complete (22 times bath volume) after 7 min.
33. P. Fatt and B. L. Ginsborg, *J. Physiol.* **142**, 516 (1958).


34. We thank H. C. Lee and A. Galione for cADPR and R. F. Irvine for $InsP_3$. Supported by the Biotechnology and Biological Sciences Research Council (grant PG87/529 to D.S.).

5 October 1994; accepted 16 February 1995